

The nature of the KW object[★]

R. Chini¹, V. H. Hoffmeister¹, K. Kämpgen¹, S. Kimeswenger², M. Nielbock¹, and R. Siebenmorgen³

¹ Astronomisches Institut der Ruhr-Universität Bochum, Universitätsstrasse 150/NA 7, 44780 Bochum, Germany
e-mail: chini@astro.ruhr-uni-bochum.de

² Institut für Astrophysik, Leopold-Franzens-Universität Innsbruck, Technikerstrasse 25, 6020 Innsbruck, Austria

³ European Southern Observatory, Karl-Schwarzschild-Strasse 2, 85748 Garching, Germany

Received 15 January 2004 / Accepted 2 August 2004

Abstract. The KW object, which has been one of the most puzzling infrared sources for three decades, has been resolved into a system of two early B-type stars with a projected separation of 2600 AU. While the more luminous component shows a huge IR excess due to circumstellar dust, the fainter one displays X-ray emission. The system is deeply embedded ($A_V \sim 24$ mag) in the molecular cloud M 17 SW and associated with an IR reflection nebula. A radiative transfer model of the spectral energy distribution of the IR excess object requires a stellar source of $5.1 \times 10^3 L_\odot$ – equivalent to a B0 star – surrounded by $10 M_\odot$ of circumstellar material. The KW object is associated with a small cluster of about 150 red stars. The stellar density within 0.1 pc is $>2.4 \times 10^3 \text{ pc}^{-3}$. From all new evidence we suggest that the KW object is one of the youngest, most deeply embedded Herbig Be stars known to date.

Key words. stars: formation – stars: circumstellar matter – stars: pre-main sequence – infrared: stars – Galaxy: open clusters and associations: general

1. Introduction

Three decades ago Kleinmann & Wright (1973) discovered a strong 10 and 20 μm source in the molecular cloud M 17 SW and speculated that it might be a dusty source with a colour temperature of about 200 K. Henceforth the object was the subject of several investigations and received numerous labels like M 17 IRS, M 17 SW, M 17 IRS1 or the Kleinmann-Wright (KW) object. Its nature, however, remained puzzling.

Tokunaga & Thompson (1979) observed strong $\text{Br}\gamma$ emission from the region, which – in the case of a compact HII region – requires a B0 ZAMS star for its excitation. The observed 1–20 μm luminosity of the KW object, however, was a factor of 10 too low. Therefore, they suggested that the $\text{Br}\gamma$ line might be due to the ionisation by a small cluster. In contrast, Dyck (1982) concluded from slit scans at 2.2 and 3.8 μm that there is no extended structure and claimed that the KW object is a compact source of less than $0''.5$ in diameter. Further $\text{Br}\gamma$ studies (Simon et al. 1981) have been interpreted in terms of an optically thick outflow ($\dot{M} > 10^{-6} M_\odot \text{ yr}^{-1}$) with a blue-shifted velocity component relative to the ambient medium. The wind hypothesis was put forward by several other authors – among them Persson et al. (1984) ($2.2 \times 10^{-6} M_\odot \text{ yr}^{-1}$) and Jinliang et al. (1997) ($1.3 \times 10^{-6} M_\odot \text{ yr}^{-1}$) – and was supported by the upper limits of the radio emission at 1.3, 6 and 21 cm (Felli et al. 1984). Simon et al. (1983) found variability of

the $\text{Br}\alpha$ emission and suggested that the region may contain at least an optically thin and an optically thick HII region where the latter is producing the IR line radiation. Eventually, Bunn et al. (1995) speculated that the IR recombination line profiles of the KW object resemble those of a deeply embedded Herbig Be star. Since then no further attempt has been made to clarify the nature of this source.

The above results leave us with a relatively confused picture of the KW object as concerns its spectral type, extinction, variability, multiplicity as well as the presence of a wind, a compact HII region and a small cluster. In the following, we describe recent observations of the region, which shed new light on this peculiar source and resolve some of the ambiguities.

2. Observations

The JHK_s imaging was carried out in September 2002 with ISAAC at the ESO VLT. The pixel resolution of $0''.15$ was degraded by seeing to about $0''.5$, the 10σ limiting magnitudes are $J = 22.8$, $H = 21.8$ and $K_s = 20.7$; details of the reduction process will be described elsewhere (Hoffmeister et al., in preparation). The MIR imaging between 3.9 and 17.8 μm and the spectroscopy of the silicate absorption feature was performed with TIMMI2 at the ESO 3.6 m in July 2003 and has been reduced with the package MOPSI. The seeing was $0''.7$; the slit width for spectroscopy was $1''.2$. The quoted flux densities have errors of about 15% (L, M), less than 10% ($N1, N10.4$) and 25% ($Q1$). In addition, we re-measured several MIR fluxes

[★] Based on observations collected at the European Southern Observatory, La Silla, Chile.

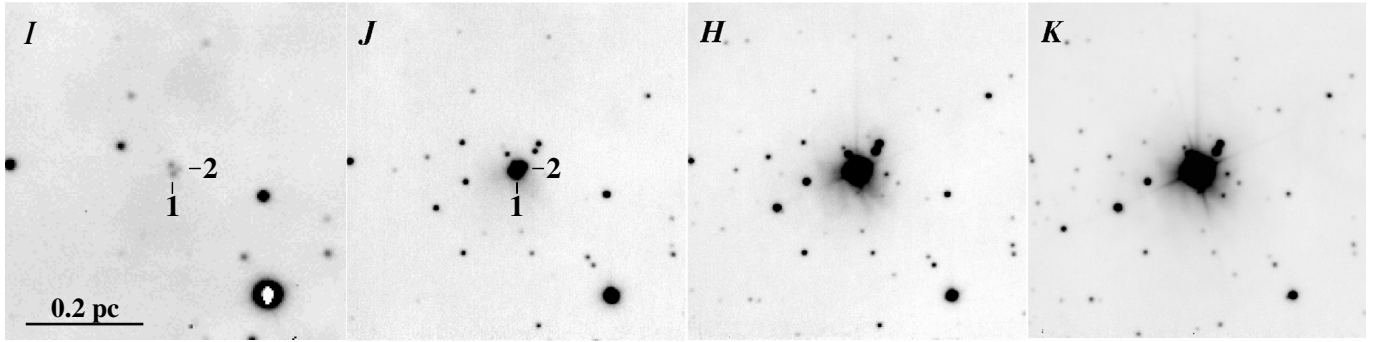


Fig. 1. $iJHK_s$ images of the KW region. The components of the KW object, which could be resolved from i to K_s , are marked by numbers; the size of the displayed area is $55'' \times 55''$.

Table 1. Multi-colour photometry of the KW object components Nos. 1 and 2.

	0.8	1.25	1.65	2.2	3.9	4.6	8.3	8.6	10.4	12.1	14.7	17.8	21.3	$[\mu\text{m}]$
No. 1	2.5E-2	7.1	91	550										
No. 2	1.1E-2	2.6	17	32	4398	5772	22 782*	30 941	26 491	32 600*	33 074*	55 488	68 762*	[mJy]

Flux densities marked with “*” were recalculated from the MSX archive.

from the MSX archive. The calibration was done according to the MSX manual without colour corrections whose effects are only significant for very cold sources. The corresponding errors are of the order of 5%. A complementary Gunn i band image ($\lambda = 806$ nm) of the region was taken with EMMI at the ESO NTT in July 2003; the limiting magnitude of this 5 minute exposure is $i \sim 23$ and the photometric errors are $\leq 10\%$ for the faintest stars in the field. Figure 1 displays the investigated area around the KW object at $iJHK_s$. The positions of stars Nos. 1 and 2 are 18:20:19.44, $-16:13:30.6$ and 18:20:19.37, $-16:13:29.8$ (J2000), respectively.

3. Source properties

3.1. Morphology

The i band image of Fig. 1 shows three faint sources in the field center which coincide with the position of the KW object. On the basis of its blue colour, the most northern one is probably unrelated to the complex. The J band image shows the two remaining objects as bright IR sources with a separation of $1''.2$, equivalent to a projected distance of 2600 AU at a distance of 2.2 kpc. Figure 3 classifies both sources as heavily embedded objects ($A_V \sim 24$ mag), with source No. 1 exhibiting a strong IR excess; No. 2 shows X-ray emission (K. Getman, private communication). Given the fact that these objects are by far the brightest K band sources within 2.4×10^5 AU, their projected spatial coincidence and similar high extinction suggest that they may form a bound system. Both stars are surrounded by an IR reflection nebosity.

3.2. Photometry

The photometry of the KW object components is given in Table 1. The i and JHK_s fluxes have been resolved for the first time and can be uniquely assigned to the individual

components. At longer wavelengths the spatial resolution is not sufficient to discriminate between Nos. 1 and 2; due to both the NIR brightness and the K band excess of No. 1, however, we assume that most of the MIR flux originates from this source. There is a large amount of K band data which vary by several tenths of magnitudes, however, there is no obvious systematic trend: 2MASS gives $K = 7.2$ for the combined KW object compared with 7.7 from this paper for instance. At $\lambda > 2.2 \mu\text{m}$, different bandpasses and apertures prevent any reasonable comparison.

3.3. Circumstellar environment

Estimates of the visual extinction toward the KW object were given by Tokunaga & Thompson (1979) ($A_V > 11.8$) and McGregor et al. (1984) ($A_V = 14.5$). Alonso-Costa & Kwan (1989) and Jinliang et al. (1997) used published $\text{Br}\alpha$, $\text{Br}\gamma$ and $\text{P}\gamma$ fluxes and calculated $A_V = 18 \pm 4$ and 20 ± 4.9 , respectively. Eventually Porter et al. (1998) obtained $A_V \approx 27$ from both the continuum and the HI lines. Using the present J and H data we obtain $A_V \sim 30$ and 24 mag for Nos. 1 and 2, respectively. The NIR colours for both components are compatible with early B-types.

Figure 2 shows the first quasi-simultaneous broad-band spectral energy distribution of the KW object from 0.8 to $21 \mu\text{m}$ together with the TIMMI 2 $10 \mu\text{m}$ spectrum and the ISOCAM CVF spectrum retrieved from the ISO archive. The solid curve is the result of a one-dimensional radiative transfer model as described by Siebenmorgen et al. (2001) which uses a standard mixture of silicate and graphite particles plus very small particles with sizes of $\approx 5 \text{ \AA}$. Two basic quantities, the total observed luminosity and the visual extinction as determined by the optical/NIR spectral slope, constrain the remaining parameters of the model fairly well. A reasonable fit has been achieved with a central source of $T = 25\,000$ K and a luminosity

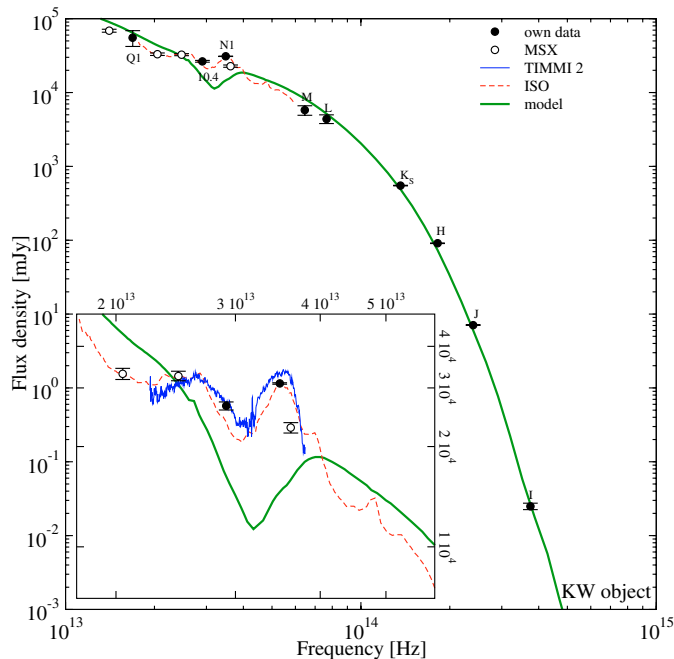


Fig. 2. The first quasi-simultaneous SED of the KW object (component 1) with the TIMMI 2 (slit width $1''.2$) and ISOCAM CVF ($6'' \times 6''$ pixel) spectra included. The solid curve is a model fit assuming a constant spherical dust distribution.

of $5.1 \times 10^3 L_{\odot}$; this corresponds to a B0 star, corroborating our result from the NIR colours.

The circumstellar emission requires a dusty cocoon of 0.1 pc in radius which corresponds to the size of the IR reflection nebula; the radial density profile was assumed to vary with $r^{-0.5}$. This configuration yields a total circumstellar mass of $10 M_{\odot}$ and produces a visual extinction of $A_V = 12$ mag. In order to match the optical/NIR slope of the SED, another 8 mag of foreground extinction are required. Such a “cold screen” between the source and the observer is also indicated by the gap in Fig. 3 which separates moderately reddened stars of $(J - H) < 1.0$ – equivalent to $A_V < 8$ mag for an early type star – from deeply embedded objects ($(J - H) > 1.5$).

The silicate feature cannot be reproduced by the normal abundances in our model (see insert in Fig. 2). The observed absorption feature suggests a visual extinction of 8.5 mag when using the standard relation $\tau_V \sim 18 \cdot \tau_{0.7}$ (Krügel 2002). This extinction is probably due to the interstellar dust on the line of sight as mentioned above. The absence of any silicate absorption from the circumstellar material might be due to larger-than-normal grains – frequently observed with Herbig Ae/Be stars (e.g. Hernández et al. 2004) – or a particular dust composition (e.g. grain destruction at $T > 1500$ K) both of which would suppress the silicate resonance. Likewise, emission from crystalline silicate – as observed in other Ae/Be stars (Waelkens et al. 1996) – might “fill up” any absorption feature. Another explanation could be a disk-like configuration which also produces silicate features both in emission and absorption (e.g. Chiang & Goldreich 1997) depending on the disk orientation.

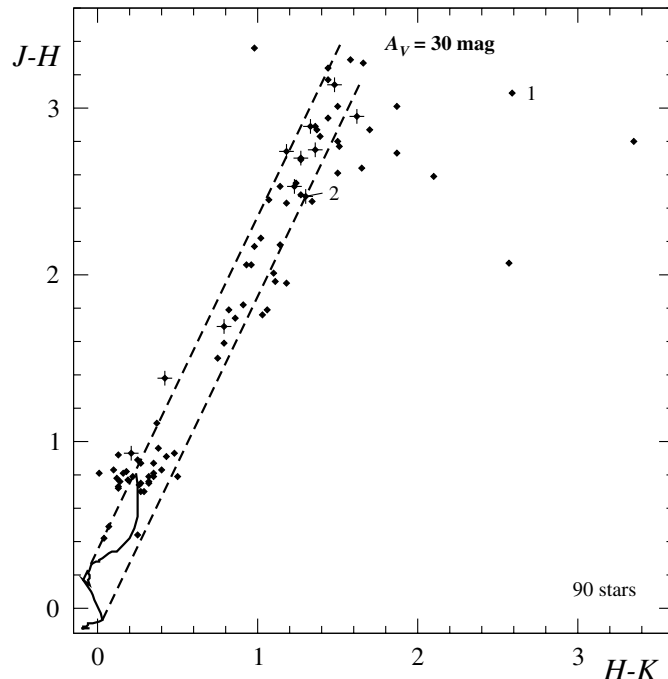


Fig. 3. *JHK* diagram for 90 stars within ~ 0.7 pc from component 1. Stars labelled “1” and “2” designate the two components of the KW object, crosses mark X-ray sources. The curve displays the unreddened main sequence (Ducati et al. 2001), the dashed lines denote the abnormal reddening path within M 17 (Hoffmeister & Chini 2003).

The observed PAH emission is much smoother than what is expected from “normal” ISM conditions; therefore, we did not include this option in our model fit. Similar features are seen in protoplanetary disks where the UV radiation field is strong and where the emission might be attributed to carbonaceous grains. It should be noted, however, that the absence of PAHs is observed in several other Herbig Ae/Be stars with substantial IR excess.

3.4. The stellar neighbourhood

The molecular cloud M 17 SW is extremely opaque at the location of the KW object: Thronson & Lada (1983) determined A_V values of about 200 and 240 mag from the column densities of ^{13}CO and $^{12}\text{C}^{18}\text{O}$, respectively. Therefore it is likely that the environment of the KW object is completely shielded against any contamination from background stars. Nevertheless, there is a small concentration of mostly red stars that stands out from the generally empty field of the molecular cloud. In order to determine whether there is a physical association among the objects we use the visual extinction as a discriminator.

Figure 3 shows the NIR colour–colour diagram of 90 sources within 0.7 pc from the KW object for which *JHK* data could be obtained. There is a pronounced gap between $1.0 < J - H < 1.5$ mag separating 35 low-reddened ($A_V < 7$ mag) from 55 deeply embedded sources. Several of them show evidence for IR excess, one of the largest occurring with the KW object itself. An additional 39 stars – detected only at *H* and *K* – have $20 < A_V < 76$ mag, suggesting that they are further members of the aggregate; extreme A_V values, however,

may be simulated by excess emission at K . Eventually, there are 46 objects detected only at K ; their $H - K$ limits indicate that they are at least as red as the other embedded stars. Thus, the KW object is located toward the projected center of an aggregate of about 150 heavily reddened objects which is simultaneously a local maximum of IR excess sources. Comparing the positions of Chandra sources in this field (K. Getman, private communication), we find 29 X-ray sources of which 17 coincide with our NIR sources.

From the $J/J-H$ and $H/H-K$ colour-magnitude diagrams, crude spectral types may be estimated by shifting 95 heavily reddened stars onto the zero-age main sequence; for those stars with JHK data we prefer the results from the $J/J-H$ diagram to minimize the effect of K band excess emission. This procedure yields $\sim 50\%$ B and $\sim 20\%$ A and F types, respectively. Due to the large and variable extinction no completeness estimates can be made; likewise, any excess emission will simulate an earlier spectral type. The average stellar density is 75 stars pc^{-3} for $r < 0.7$ pc increasing to 2.4×10^3 stars pc^{-3} for the B stars within the central 0.1 pc.

4. Discussion

In the following we combine all observational evidence to argue that the KW object is the most heavily embedded Herbig Be star associated with a small stellar group.

The KW object fulfills all definitions of a Herbig Be star as there are (a) spectral type B with emission lines; (b) located in an obscured region; and (c) bright nebulosity in its immediate vicinity (Herbig 1960). It also complies with the more recent working definition which additionally includes IR excess due to circumstellar dust (Waters & Waelkens 1998) and a location outside a complex star forming region.

We have resolved the KW object into two components of early B-type stars which may form a binary system. Binarity is a frequent property of early type stars but has been observed particularly with Be stars, too (Li et al. 1994). The extinction towards the system is about 24 mag indicating that the KW object is by far the most deeply embedded Be star; typical A_V -values found with Ae/Be stars are below 5 mag (Hillenbrand et al. 1992; Testi et al. 1999).

Whether the X-ray emission of the fainter IR component is due to a stellar wind or originates from an invisible low-mass TTauri companion cannot be decided from the present data. The stronger IR component, however, is most likely one of the youngest Herbig Ae/Be star ever found: its steep SED, dominated by circumstellar matter, classifies the source as an extreme member of *Group II* (Hillenbrand et al. 1992) or as an extreme class I object with a spectral slope of $\alpha = 1.5$ (e.g. Lada & Adams 1992). In both cases, the corresponding YSOs are interpreted as star/disk or protostellar systems with dominating envelopes where a substantial fraction of the luminosity originates from accretion. Obviously, classification schemes based on infrared energy distributions refer to the warm dust emission close to the star and do not take into account the influence of extinction which may severely steepen the spectral slope. Another classification, based on the amount of cold circumstellar material, has been proposed by Fuente et al. (1998).

Circumstellar disk/envelope masses around Herbig Ae/Be stars are usually obtained from the millimetre continuum or from molecular lines. Although included in a 1.2 mm survey of the M 17 region, the KW object does not show up as an individual source within the huge extended emission from the HII region/molecular cloud complex (Chini et al., in preparation). Hillenbrand et al. (1992) report typical masses in the range $0.01 < M_{\text{env}}[M_{\odot}] < 1$ with an exceptionally high value of 5.8 for LkH α 234. Based on ^{13}CO , C^{18}O and 1.3 mm continuum data Fuente et al. (2002) find masses between $\leq 0.02 < M_{\text{env}}[M_{\odot}] < 16.6$ within a radius of 0.08 pc from the central star; the largest value of $16.6 M_{\odot}$ refers again to LkH α 234. Given that all these mass estimates have uncertainties of at least a factor of two, the circumstellar mass derived from our model fit for the KW object is in the upper range of envelopes observed around Herbig Be stars. This also corroborates the youth of the KW object because the mass dispersal of dense gas around early-type Be stars is extremely efficient (Fuente et al. 1998).

The optical continuum of Herbig Be stars can be variable on several time scales, indicating different physical mechanisms (e.g. Harmanec 1998); likewise, line variations have been documented in many cases (e.g. Pogodin 1994). Here, the K band variability and the variation in the Bry line strength (Simon et al. 1983) of the KW object fit into the general picture of a Herbig Be star.

Finally, Herbig Be stars tend to be surrounded by dense clusters of lower mass companions whose richness depends on the spectral type of the Be star (Hillenbrand et al. 1995; Testi et al. 1999). The most massive stars are associated with clusters of volume densities between $10^2 - 10^3 \text{ pc}^{-3}$ in agreement with the present results. With a size of about 0.7 pc, the KW object – together with MCW 1080 (Testi et al. 1999) – belongs to the largest clusters found so far. We therefore suggest that the KW object is the central, most massive object within a new cluster that has recently formed.

Acknowledgements. This work was partly funded by the Nordrhein-Westfälische Akademie der Wissenschaften.

References

- Alonso-Costa, J. L., & Kwan, J. 1989, *ApJ*, 338, 403
- Bunn, J. C., Hoare, M. G., & Drew, J. E. 1995, *MNRAS*, 272, 346
- Chiang, E. I., & Goldreich, P. 1997, *ApJ*, 490, 368
- Ducati, J. R., Bevilacqua, C. M., Rembold, S. B., & Ribeiro, D. 2001, *ApJ*, 588, 309
- Dyck, H. M. 1980, *AJ*, 85, 891
- Fuente, A., Martin-Pintado, J., Bachiller, R., Neri, R., & Palla, F. 1998, *A&A*, 334, 253
- Fuente, A., Martin-Pintado, J., Bachiller, R., Rodriguez-Franco, A., & Palla, F. 2002, *A&A*, 387, 977
- McGregor, P. J., Persson, S. E., & Cohen, J. G. 1984, *ApJ*, 286, 609
- Felli, M., Churchwell, E., & Massi, M. 1984, *A&A*, 136, 53
- Harmanec, P. 1998, *A&A*, 337, 183
- Herbig, G. H. 1960, *ApJS*, 4, 337
- Hernández, J., Calvet, N., Briceno, C., Hartmann, L., & Berlind, P. 2004, *AJ*, 127, 1682
- Hillenbrand, L. A., Meyer, M. R., & Strom, S. E. 1995, *AJ*, 109, 280

- Hillenbrand, L. A., Strom, S. E., Vrba, F. J., & Keene, J. 1992, *ApJ*, 397, 613
- Hoffmeister, V. H., & Chini, R. 2003, in *Open Issues in Local Star Formation*, ed. L. Lépine, & J. Gregorio-Hetem (Kluwer Academic Publishers), *ASSL*, 299
- Jinliang, H., Dongrong, J., & Chengqui, F. 1997, *A&A*, 327, 725
- Kleinmann, D. E., & Wright, E. L. 1973, *ApJ*, 185, L133
- Krügel, E. 2002, in *The Physics of Interstellar Dust, Series in Astronomy and Astrophysics* (Bristol and Philadelphia: Institute of Physics Publishing)
- Li, W., EvansII, N. J., Harvey, P. M., & Colomé, C. 1994, *ApJ*, 433, 199
- Lada, C. J., & Adams, F. C. 1992, *ApJ*, 393, 278
- Persson, S. E., Geballe, T. R., McGregor, G. J., Edwards, S., & Lonsdale, C. J. 1984, *A&A*, 286, 289
- Porter, J. M., Drew, J. E., & Lumsden, S. L. 1998, *A&A*, 332, 999
- Pogodin, M. A. 1994, *A&A*, 282, 141
- Siebenmorgen, R., Krügel, E., & Laureijs, R. 2001, *A&A*, 377, 735
- Simon, M., Felli, M., Cassar, L., Fischer, J., & Massi, M. 1983, *ApJ*, 266, 623
- Simon, M., Righini-Cohen, G., Fischer, J., & Cassar, L. 1981, *ApJ*, 251, 552
- Testi, L., Palla, F., & Natta, A. 1999, *A&A*, 342, 515
- Thronson, H. A., & Lada, C. J. 1983, *ApJ*, 269, 175
- Tokunaga, A. T., & Thompson, R. I. 1979, *ApJ*, 229, 583
- Waelkens, C., Waters, L. B. F. M., de Graauw, M. S., et al. 1996, *A&A*, 315, L245
- Waters, L. B. F. M., & Waelkens, C. 1998, *ARA&A*, 36, 233